Analysis of Novel Helmholtz-inductively Coupled Plasma Source and Its Application for Nano-Scale MOSFETs

Kun-Joo Park*, Kee-Hyun Kim, and Weon-Mook Lee
DMS Co., Ltd, #402, Sungshin Techno-Park Building 509-7, Suwon 443-803, Republic of Korea

Heeyeop Chae
Department of Chemical Engineering, SungKyunKwan University, Cheoncheon-dong, Jangan-gu, Suwon 440-746, Republic of Korea

In-Shik Han and Hi-Deok Lee
Department of Electronics Engineering, Chungnam National University, Gung-dong, Yuseong-gu, Daejeon 305-764, Republic of Korea

(Received January 16 2009, Accepted April 13 2009)

A novel Helmholtz coil inductively coupled plasma (H-ICP) etcher is proposed and characterized for deep nano-scale CMOS technology. Various hardware tests are performed while varying key parameters such as distance between the top and bottom coils, the distance between the chamber ceiling and the wafer, and the chamber height in order to determine the optimal design of the chamber and optimal process conditions. The uniformity was significantly improved by applying the optimum conditions. The plasma density obtained with the H-ICP source was about $5\times10^{11}/cm^3$, and the electron temperature was about 2–3 eV. The etching selectivity for the poly-silicon gate versus the ultra-thin gate oxide was 482:1 at 10 sccm of HeO_2. The proposed H-ICP was successfully applied to form multiple 60-nm poly-silicon gate layers.

Keywords: Inductively coupled plasma, Plasma density, Gate etching, Nano process

1. INTRODUCTION

As the minimum feature size of the metal-oxide semiconductor field effect transistor (MOSFET) has shrunk to the nano-scale regime, fine patterning with plasma etching has become crucial in fabricating ULSI devices[1,2]. The most popular plasma sources for the formation of a nano-scale poly-silicon gate and shallow trench isolation are capacitively coupled plasma (CCP) and inductively coupled plasma (ICP) sources. Typically, CCP sources provide relatively low to medium plasma density (10^{10}–$10^{11}/cm^3$) with good uniformity. However, a major limitation of the CCP source is the difficulty in controlling the plasma density and the ion energy independently. By contrast, ICP sources both provide a high-density plasma and offer the capability of controlling the plasma density and the ion energy independently, which has made these sources more popular than CCP. Other high-density plasma sources have been developed for various applications and for next-generation MOSFET technology[3-5], but they are not as popular as CCP or ICP because it is hard to obtain good uniformity across large wafers(> 300 mm)[6].

In this work, we propose a novel Helmholtz inductively coupled plasma (H-ICP) source for plasma etching with high uniformity and a high selectivity that is suitable for nano-scale semiconductor devices. Various kinds of hardware and process split were applied, and the optimum condition was successfully applied for the formation of nano-scale poly-silicon gates.

2. EXPERIMENT

Figure 1 provides a schematic diagram of the proposed H-ICP plasma chamber. A homogeneous magnetic field, B, is produced by a pair of conducting circular coils which are separated by a distance almost equal to the radius of the circular loops. Each coil has N turns, and an electromagnetic field (EMF) is produced in the center area between the two circular coils. The generated magnetic flux density, B, at the midpoint between the coils is given by (1), where R is the radius of coil, I is current flowing through the coil, n is the number of turns in each coil, and μ_0 is the permeability constant.

$$B=\left(\frac{4}{5}\right)^{3/2}\frac{\mu_o nI}{R} \tag{1}$$

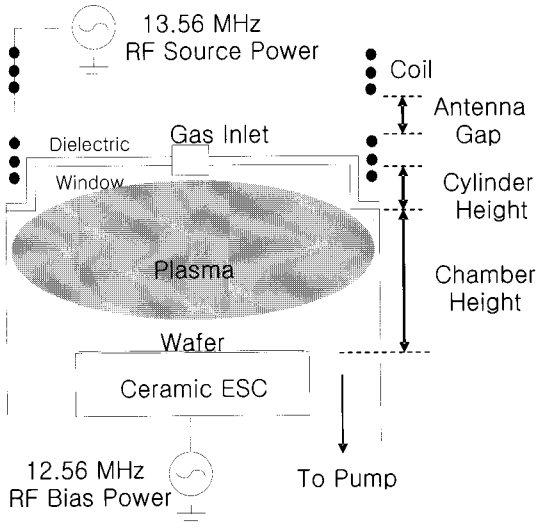

Fig.1. Schematic diagram of the H-ICP system.

*Author to whom corresponding should be addressed: electronic mail: kjpark@dms21.co.kr

Table 1. Key process conditions for optimization of the H-ICP chamber reactor.

Items for H-ICP Chamber		Plasma	Analysis	Results
Antenna Gap	Standard	Ar	Plasma potential Electron temperature Ion density Electron density	Etch rate Uniformity De-coupling effect Final profile
	20 % down	HBr		
	40 % down	Cl_2		
	60 % down			
Chamber Height	Standard	Ar		
	20 mm up	HBr		
	40 mm up	Cl_2		
	60 mm up			
Cap Height	Standard	Ar		
	Half	HBr		
		Cl_2		

Table 2. Characteristics of the etch rate and the uniformity in the H-ICP chamber for various hardware configurations.

No.	Cap height	Chamber height	Antenna gap	ICF uniformity			Main Etch rate / uniformity	Over Etch rate / uniformity
				Ar	Cl_2	HBr		
1	Standard	Standard	20 % down	14.6	14.4	6.2	4532 / 4.8	2502 / 2.0
2	Half	20 mm up	20 % down	12.2	13.0	7.8	3894 / 4.3	1843 / 3.2
3	Half	40 mm up	20 % down	13.5	15.0	8.5	4296 / 4.3	2235 / 1.3
4	Half	60 mm up	20 % down	14.5	16.3	14.7	4114 / 4.2	1958 / 3.0
5	Half	Standard	20 % down	11.9	10.8	4.4	3862 / 4.1	2145 / 2.0
6	Half	Standard	40 % down	11.0	11.3	4.2	3856 / 4.1	2114 / 2.0
7	Half	Standard	60 % down	12.3	11.1	4.0	3926 / 3.8	2172 / 3.7
8	Half	Standard	Standard	11.1	11.1	5.2	3723 / 5.0	1867 / 2.5

According to the Helmholtz theory, the most uniform magnetic flux density lies at the center point between the coils[7]. In practice, though, it is difficult to place a ceramic electrostatic chuck (ESC) at this center position because of the various hardware constraints. Therefore, it is important to precisely control the space between the inductive coils (antenna gap) and the chamber height in order to obtain the conditions for a uniform plasma.

Radio-frequency (RF) power at 13.56 MHz is applied to the coils located above the ceramic cover, and a second source of RF power (at 12.56 MHz) is applied to the cathode equipped with the ESC, which is thermally controlled using helium backside cooling. The chamber is evacuated with a 2300-l/s turbo-molecular pump backed by a dry mechanical pump. Process gases are introduced from a top gas inlet through the center of the dielectric window at a controlled flow rate, and the chamber pressure is controlled with the throttling gate valve (TGV).

We used a double Langmuir probe (Plasmart DLP2000^{TM}) to characterize the H-ICP in this study. Table 1 summarizes the test conditions, such as plasma types, the antenna gap, the chamber height, and the cap, or cylinder, height. The items used for analysis and plasma output are also summarized in Table 1, and the test conditions for each parameter are listed along with the "standard" condition as a reference. We used 200-mm wafers with 620-Å BARC, 2700-Å ArF PR, and 1600-Å poly silicon on 15-Å gate oxide for our etching experiments. The poly-silicon etch rate and the uniformity were measured using a K-MAC (Korea Materials & Analysis Corp. ST5000A), and the cross-sectional profiles were analyzed with a scanning electron microscope (Hitachi S-5000).

3. RESULTS AND DISCUSSION

The average etch rate (Å/min) and uniformity (%) for the various test conditions listed in Table I are summarized in Table II; the final chamber condition was fixed as a 20 % reduction of antenna gap, standard chamber height, and half the cap height. Figure 2 shows the ion current flux (ICF) density (mA/cm^2) and the ICF uniformity as a function of RF power for various chamber heights and antenna gaps; the Ar plasma was set at 5 mTorr, and the Ar flow rate was 100 sccm. The ICF density increases as the source power increases, indicating a strong dependence of the ion density on the source power. The increased ion flux density is typically attributed to enhanced plasma density, radicals, and ions.

Figure 3 shows how the ion current flux varies with different antenna gaps at various RF power settings under a Cl_2 plasma. As can be seen, the ICF is strongly dependent on the antenna gap in addition to being dependent on the source power. Figure 4 shows how the ICF density varies with different chamber heights and antenna gaps, where the chamber pressure ranges from 10 mTorr to 70 mTorr, the RF source power is 1000 W, and the HBr plasma has a flow rate of 100 sccm. As the processing pressure of the HBr plasma increases, the ICF decreases. When the antenna gap

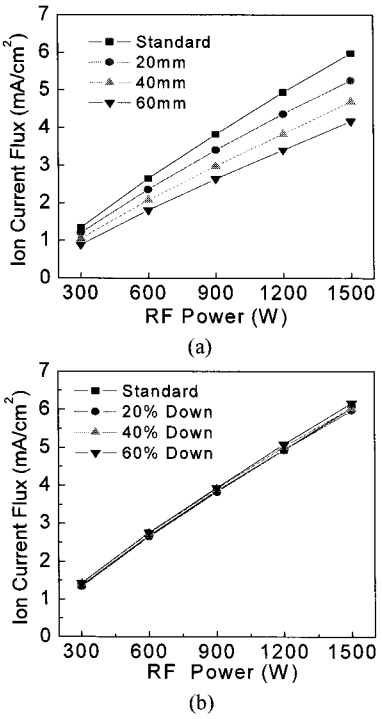

Fig. 2. Ion current flux (ICF) density as a function of the RF power with a split of (a) chamber height and (b) antenna gap. Ar pressure is 5 mTorr.

is dropped below the standard, there were no big difference in the ICF. On the other hand, as the chamber height increases, the ICF decreases and the ICF uniformity (%) has been improved because of the recombination of ions during the diffusion from the bulk plasma to the wafer surface.

As shown in Fig. 5, we analyzed ICF uniformity within the wafer for both the Cl_2 and HBr plasmas. The chamber pressure, RF source power, and gas flow rate were, respectively, 5 mTorr, 1000 W, and 100 sccm for the Cl_2 plasma and 50 mTorr, 1000 W, and 100 sccm for the HBr plasma. In both cases the ICF uniformity decreases as the height decreases. It is noteworthy that the ICF decreases abruptly at the center region in the case of a half cap for the HBr plasma, which results in a 5.2 % improvement in the uniformity, as compared to the 13.8 % improvement in the case of a 63-mm height.

The difference in ICF between the Cl_2 and HBr plasmas seen at the wafer center in Figs. 5 and 6 can be explained in terms of the etching yield. It is well known that bromine-based chemistry is commonly used for etching in order to achieve high selectivity and anisotropic etching, while Cl_2 is added to increase the etching rate[8]. As proposed by Jin et al., the spontaneous etching of silicon with Ar, Cl_2, and HBr is negligible, but the etching yield is greatly enhanced by ion bombardment[9]. The etching yield of silicon (i.e., the number of Si atoms removed per incident ion) as a function of ion energy, ion impingement angle, and ion current flux is a crucial parameter for the etching process. Thus the etching yield in pure Cl_2 plasma is greater than in HBr plasma, probably because of differences of formation energy and boiling point between Cl_2 and HBr[10].

In case of the HBr plasma, as Fig. 5 shows, when the chamber height is varied, the ICF is decreased at the wafer center only for the half cylinder case; by contrast, when the antenna gap is varied, as show in Fig. 6(b), all of conditions show a lower ICF, which points to one of the characteristics of H-ICP: a high ICF at the wafer center over a certain threshold, and a low ICF under the threshold. This variation in the ICF indicates that the ICF uniformity as a function of the antenna gap improves the uniformity of etching process.

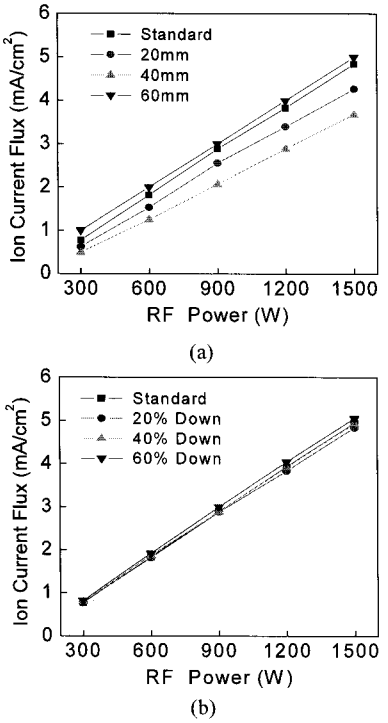

Fig. 3. Dependence of ion current flux (ICF) density on (a) chamber height and (b) antenna gap in the case of the Cl_2 plasma with a Cl_2 pressure of 5 mTorr.

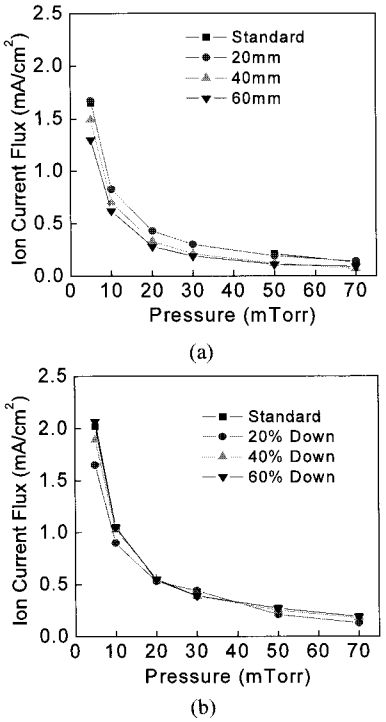

Fig. 4. Ion current flux (ICF) density as a function of the chamber pressure under HBr plasma with a RF source power of 1000 W for various (a) chamber heights and (b) antenna gaps.

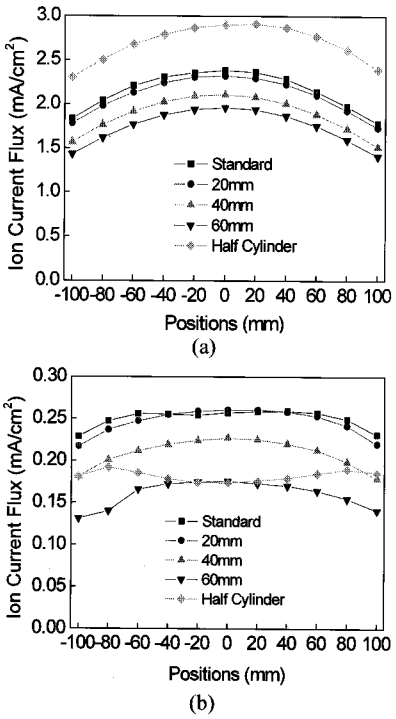

Fig. 5. Comparison of the uniformity of ion current flux (ICF) density as the chamber height is varied, in the case of (a) Cl_2 plasma, and (b) HBr plasma.

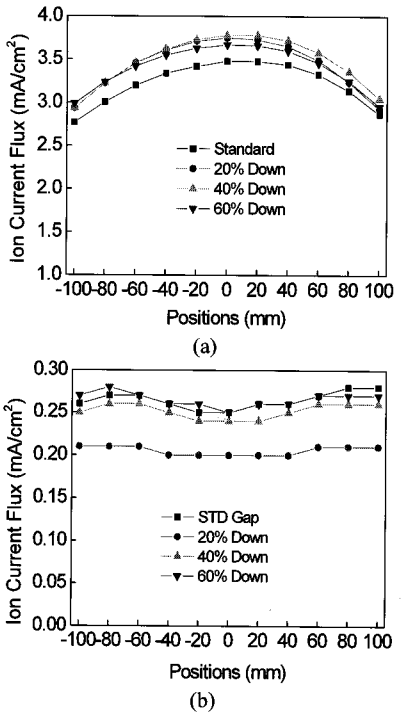

Fig. 6. Dependence of the uniformity of the ion current flux (ICF) density on the antenna gap for the case of (a) Cl_2 plasma and (b) HBr plasma. The chamber pressure, RF source power, and gas flow rate are, respectively, 5 mTorr, 1000 W and 100 sccm for the Cl_2 plasma and 50 mTorr, 1000 W, and 100 sccm for the HBr plasma.

This is believed to be due to the decoupling effect, and it is desirable for achieving a high etching selectivity for the gate versus the ultra-thin gate oxide. As the antenna gap is varied, as shown in Fig. 6, the HBr plasma has a more uniform ICF profile than the Cl_2 plasma. Furthermore, an HBr plasma has advantages in nano-scale device formation because the etch damage can be lowered and the selectivity can be improved thanks to its low ion density. Therefore, we fixed the final process condition to be a 20 % reduction in the antenna gap from the standard height of the chamber and half the cylinder height. The plasma density obtained with the H-ICP source is about 5×10^{11} /cm^3, and the electron temperature is about 2~3 eV. We found that the etching selectivity for the poly-silicon versus the ultra-thin gate oxide is 482:1 with 10 sccm of HeO_2, which is high enough for gate patterning in nano-scale MOSFET technology.

As shown in Fig. 7, we applied the optimum etching conditions for a nano-scale poly-Si gate to 65-nm technology with 620-Å BARC, 2700-Å ArF PR, and 1600-Å poly-silicon on a 15-Å gate oxide. There was little variation in gate length or cross-sectional profile between the isolated and the dense gates for either the top or the center regions of the wafer. No active damage occurred even with an ultra-thin gate oxide of 15 Å, and the remaining ArF PR is about 1000 Å. Figure 7 also shows a very steep gate profile with a slope of about 89-90 degree. The misaligned ArF PR from the poly gate visible in Fig. 7(c) was caused during the sample preparation for SEM analysis. Therefore, the proposed H-ICP source is a promising method for the patterning of nano-scale gate layers.

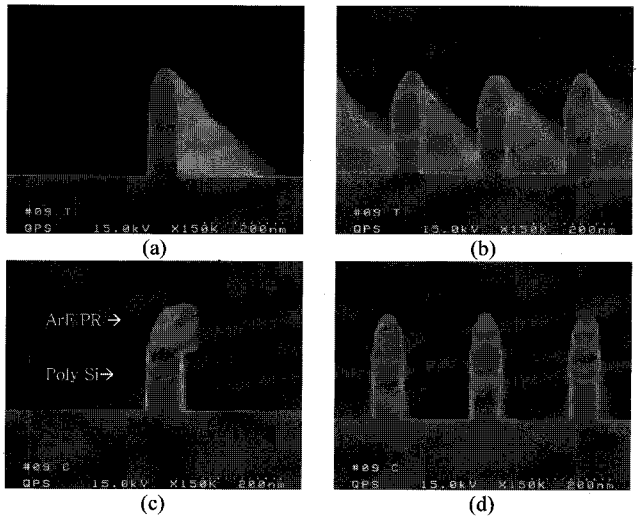

Fig. 7. Cross-sectional SEM profiles of the etched poly-silicon gate using the proposed H-ICP: (a) isolated and (b) dense profiles in the upper region of wafer, (c) isolated and (d) dense profiles in the center area of wafer.

4. CONCLUSION

We proposed a novel H-ICP source for the patterning of nano-scale poly-silicon, and we analyzed its characteristics using a Langmuir probe to optimize the plasma reactor

design. Under typical operating conditions, the ion current flux can be controlled from 0.8 mA/cm^2 to 6.0 mA/cm^2. The optimum plasma condition or chamber structure was successfully applied to form 60-nm poly-silicon gates with an ultra-thin 15-Å gate oxide. Therefore, the proposed H-ICP source is very promising for use in the fabrication of nano-scale semiconductor devices.

ACKNOWLEDGMENTS

The authors would like to thank the engineers in Hardware Development and Software Development, DMS, co. Ltd. This work was supported in part by "Commercialization Program of Nano Process Equipments" of Korea Ministry of Commerce Industry and Energy.

REFERENCES

[1] K. J. Park and W. G. Lee, Jpn. J. Appl. Phys. **41**, 930 (2002).
[2] K. N. Kim and G. Y. Yeom, J. Korean Phys. Soc. **48**, 256 (2006).
[3] S.-H. Lee and G.-H. Kim, J. Korean Phys. Soc. **49**, 726 (2006).
[4] J. W. Yeo, D. P. Kim, and C. I. Kim, J. Korean Phys. Soc. **44**, 1092 (2004).
[5] J. H. Kim, K. H. Chung, and Y. S. Yoo, J. Korean Phys. Soc. **47**, 249 (2005).
[6] G. Vinogradov, et al., Abs. 899, 206th Meeting, (2004).
[7] Halliday, Resnick, and Waker, Fundamentals of Physics (6th Edition), Chap. 30, p. 687, 700-702.
[8] M. Tuda, K. Shintani, and H. Ootera, J. Vac. Sci. Technol. A, **19**, 711 (2001).
[9] W. Jin, S. A. Vitale, and H. H. Sawin, J. Vac. Sci. Technol. A, **20**, 2106 (2002).
[10] C. C. Cheng, K. V. Guinn, I. P. Herman, and V. M. Donnelly, J. Vac. Sci. Technol. A, **13**, 1970 (1994).